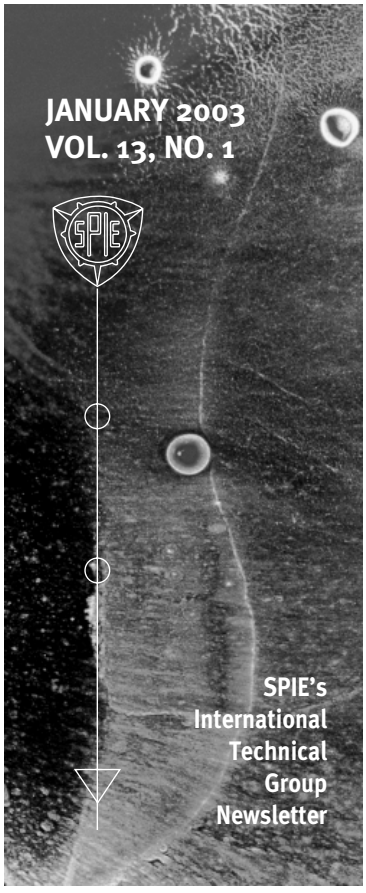

Electronic Imaging

Differential sensing of vibration for high-quality restoration of motion-blurred images

As technology advances, image quality is becoming more dependent on auxiliary factors than on the imaging system itself. Among these factors is relative motion of the camera and the object during exposure, which leads to image blur and lowers image resolution. Camera vibrations, for instance, may come from an unstable camera base—as in robotics or vehicle mounted cameras—or from other factors such as a cooling system motor incorporated into a forward-looking infra-red (FLIR) camera. In many cases vibration can be of complex non-sinusoidal form, have a spread spectrum that includes frequencies close to the frame rate, and even be non-stationary. These kinds of vibrations often lead to blur that differs considerably from frame to frame. Attempts to statistically estimate the blur result in only average restoration quality and can even destroy the image in the case of non-stationary vibrations.

This makes necessary accurate identification of the motion function and, based on it, a calculation of line spread function (LSF) unique to each frame. The more accurate the calculated LSF, the better the quality of the restoration that can be achieved. To this end, differential sensing of rotation vibrations is proposed.[1] Two dual-axis integrated accelerometers are attached to the imaging system at opposite ends and close to the optical axis as possible. The longer the distance between the sensors, the higher their output signal magnitude and dynamic range. By taking the difference of the two outputs, a signal is obtained that depends on the distance between the sensors rather than the distance from the rotation origin. Two dual-axis accelerometers provide two differential signals that represent the rotation around the two axes.

This result is highly significant for the restoration of vibration-blurred images because:

- the differential output does not depend on the location of the rotation origin, which is unknown and is subject to changes during system operation;
- consequently, the differential output gives a robust and flat response for all frequencies of vibrations, which is particularly important for systems with multiple or spread-spectrum vibration sources;
- for any given field of view, the differential output does not depend on the distance between the camera and the object; it yields pure angle information of vibrations, which can be directly (proportionally) transformed into pixels of blur;
- differential output has lower noise and larger dynamic range due to the output being summed while the noise is RMS summed; it also has a higher noise immunity to auxiliary electromagnetic interference factors.

To obtain real-world verification for the proposed differential-sensing scheme, an experimental setup was built (see Figure 1). An illuminating visible light emitting diode (LED) was set at the appropriate distance to have an image size of about two pixels in diameter. A sinusoidal wave at 23Hz frequency was supplied to an electromagnetic shaker and a few vertically vibrated images were sampled. The period of vibration (1/23Hz=43.5ms) is larger than the exposure time. This causes each video frame to have a different LSF, since blur in

Continued on page 7.

Calendar *— See page 10*

Technical Group Registration Form *— See page 11*

Newsletter now available on-line

Technical Group members are being offered the option of receiving the Electronic Imaging Newsletter electronically. An e-mail is being sent to all group members with advice of the web location for this issue, and asking members to choose between the electronic and printed version for future issues. If you are a member and have not yet received this message, then SPIE does not have your correct e-mail address.

To receive future issues electronically please send your e-mail address to:
`spie-membership@spie.org`
with the word `EI` in the subject line of the message and the words `electronic version` in the body of the message.

If you prefer to receive the newsletter in the printed format, but want to send your correct e-mail address for our database, include the words `print version preferred` in the body of your message.

Biological communication and perceptual geometry

My research group, originally named Computational and Visual Geometry (CVG) came to existence in the late 1980s, and its focus naturally evolved to research the interplay between computation, vision and geometry with emphasis on perception and the interaction between geometry and vision. These topics merge with high-performance computation to become a budding branch called perceptual geometry. The focus of perceptual geometry is to capture the way the humans—and for that matter, other animals and eventually other intelligent systems—come to form internal (probabilistic) rules: their computational strategies to cope with their environments, and to take proper actions. For living organisms, the process of forming such rules and the wet-ware to implement them finally settle into stable and highly predictable patterns of behavior. The biological process of interacting with its environment until the animal takes action (behavior), forms a memory of events (cognition), or responds with specific affective changes (as in fear and other emotion) appear to fall into a highly regular pattern with great many commonalities across individuals. The entire process could well be called biological information processing, and the set of (a priori probabilistic) rules underpinning them may well be called biological computation.

Consider the example of biological computation that underlies the formation of concepts of curvature (the bending of tree branch or a snake in contrast to straight trunk of an aspen twig) and torsion (forming a three-dimensional curvilinear shape as a spring spirals in contrast to bending all within a flat surface, as in snake's trail on sand). In Reference 1, it is shown that an intelligent system with limited memory and the capacity to infer similarities among encoded environmental stimuli from solid objects (such as visual or tactile), is capable of learning to infer quantitative measurements that would allow it to distinguish and compare curvature and torsion in elongated objects. This is, from the point of view of perceptual geometry, a geometric result with an underlying process that might well be called biological computation that manipulates the biological pieces of information within the animal's brain. What is biological computation and how can we understand and model it by conventional digital machines? This question has close connections to investigation of biological information and biological communication, and I refer the reader to my forthcoming article on the subject.[2]

I wish to comment on the modern roles of geometry and communication in image science. First, images are geometric objects. Unlike other genre in mathematics, the formation of knowledge and theories in geometry are traced back to the human perception of the physical world and the regularities within the stimuli arriving from the environment.[3-5] Helmholtz, Poincaré, and Einstein—from the classics—and J.J. Gibson, Horace Barlow, and Jan Koenderink, among the contemporaries, have developed theories and commented on their variations of what geometry means to them.[1,2,6-8] My message here is that quantum jump progress in image science depends on the depth and breadth of its integration with geometry. Secondly, image science targets two distinct yet overlapping domains. The first domain is direct use of images by humans, from the era of cave art to high-definition TV. Human perception is its main intermediary. Human intelligence is the main instrument of inference. The second domain is image science for machines and non-human autonomous agents, whether intelligent and adaptive, biologically-inspired, or organic mediated. In the second domain, the human perception has nowhere near the role that it plays in the first domain, though its interface with machine should be still an organic factor in the process.

In EI, both domains are important. Electronic media are intended, for the most part, to be used by humans, thus must be streamlined for communication with biological entities. Humans and their behavioral outputs are not disjoint from the myriad biological substrates underpinning them. On the other hand, I have argued from the point of view of evolutionary biology (inspired by Reference 9) that human behavior must be traced back to biological communication, and it could be better understood with a firmly scientifically founded theory of biological computation.[2] The practical matters in R&D of EI translate the latter into necessity of erecting a mathematical foundation for biological communication.

My final comment is on the emergence of new understanding of biological communication. Behavior is the Gestalt of communication from (statistical) integration of communication of subsystems at scales smaller than the one at hand.[2] The time-scales for completing message passing in sub-behavioral levels (that is, strictly, smaller-scale complex subsystems) are typically smaller than the scale for average behavioral time intervals. This formulation of behavior leads to a number of useful observations. For example, to optimize communication through behavior of individuals requires both dynamics, energy, and learning (reinforcement, reward,…) Further, communication amongst individuals takes place at multi-level, in a multimodal fashion. Third, communication of biological information requires encoding and decoding, and could begin by attempts at imitation in the initial phase. Fourth, all biological processes underlying living mechanisms are implicitly or explicitly involved in communication at various levels, and a certain method of averaging and Gestalt outputs communication from a smaller scale to an immediately greater scale. Finally, communication through behavior is inherently quantifiable, although we might not have the means to achieve that at this point in time.

Prof. Amir Assadi
Department of Mathematics
811 Van Vleck Hall, 480 Lincoln Drive
Madison, WI 53706-1388 , USA
Phone: 608/262-3219
Fax: 608/263-8891
E-mail: ahassadi@facstaff.wisc.edu
http://www.math.wisc.edu/~assadi/
http://www.lmcg.wisc.edu/bioCVG/

References

1. A. Assadi and H. Eghbalnia, *A Learning Theoretic Approach to Perceptual Geometry in Natural Scenes,* **J. Neurocomputing 38,** pp. 1077-1085, 2001.
2. A. Assadi, *A Theory of Communication in Biology*, (preprint 2002, forthcoming in 2003).
3. H. B. Barlow, *Sensory mechanisms, the reduction of redundancy, and intelligence*, **The Mechanisation of Thought Processes,** pp. 535-539, Her Majesty's Stationery Office, London, 1959.
4. H. B. Barlow, *The Exploitation of Regularities in the Environment by the Brain*, **Brain and Behavioral Sciences 24** (3), 2001.
5. H. B. Barlow, *Cognition As Code-Breaking*, **Perception And The Physical World,** Ch. 2, pp 21-36, Eds. Dieter Heyer and Rainer Mausfeld, John Wiley and Sons, 2002.
6. A. Assadi, H. Eghbalnia, and S. Palmer, *Geometry in Mathematical Space and Perceptual Space*, **Proc. SPIE 3811,** 1999.
7. A. Einstein, *Geometry and Experience*, lecture delivered at the Prussian Academy of Sciences in 1921, reprinted in **Sidelights on Relativity,** Dover, New York, 1983.
8. Henri Poincaré, **Science and Hypothesis**, originally published 1902, Dover, New York, 1952.
9. J. T. Bonner, **The Evolution of Complexity by Means of Natural Selection**, Princeton University Press, 1988 .

Reconstruction of high-resolution images from low-resolution images

Due to hardware cost, size, and fabrication-complexity limitations, imaging systems like charge coupled device (CCD) detector arrays often provide only multiple, low-resolution, degraded images. However, a high-resolution image is indispensable for applications such as health diagnosis and monitoring, military surveillance, and terrain-mapping by remote sensing. In addition, there is the intriguing possibility of substituting expensive, high-resolution instruments—like scanning electron microscopes—with their cruder, cheaper counterparts, and then applying restoration methods to increase the resolution to that obtainable with much-more-costly equipment. Resolution improvement by applying tools from digital image processing is, therefore, a topic of very great interest.

In this article we consider the reconstruction of high-resolution images from multiple undersampled, shifted, degraded and noisy image frames. The image-acquisition scheme is important in the modeling of the degradation process. Multiple, undersampled images of a scene are often obtained by using multiple identical image sensors that are shifted relative to each other by subpixel displacements. The resulting high-resolution image reconstruction problem using a set of low-resolution images captured by the CCD image sensors is interesting because it is closely related to the design of high-definition television (HDTV) and very high-definition (VHD) image sensors. CCD image sensor arrays, where each sensor consists of a rectangular subarray of sensing elements, produce discrete images whose sampling rate and resolution are determined by the physical size of the sensing elements. Since the multiple CCD image sensor arrays are shifted relative to each other by subpixel displacements, the reconstruction of high-resolution images can be modeled by $H f = g + n$ where f is the desired high-resolution image, H is the blur matrix, g is the output high-resolution image formed from low-resolution frames, and n is the additive Gaussian noise. A schematic for low-resolution image formation is shown in Figure 1 (left). Here the blur matrix is constructed from the averaging of the pixel values (see Figure 1 (right)).

Since the matrix H described above is ill-conditioned, solution for f is constructed by applying a regularization technique that involves a regularization functional (which captures the regularity in f), and a tuning (regularization) parameter that controls the degree of regularity of the solution. Without the regularization, the high-resolution image cannot be reconstructed well. In addition, perfect sub-pixel displacements are practically impossible to realize. Correspondingly, blur operators in multi-sensor high-resolution image reconstruction are space-variant, and we need to solve a large non-Toeplitz linear system for finding the high-resolution image. We have developed a preconditioned conjugate gradient method with cosine-transform-based pre-conditioners that can solve the required linear system very efficiently. Moreover, we have extended this algorithm to movies by using frames within a movie as our low-resolution images. In Figure 2 (left), an example of a low-resolution frame captured from a movie is given. The reconstructed high-resolution image from four low-resolution movie frames is given in Figure 2 (right).

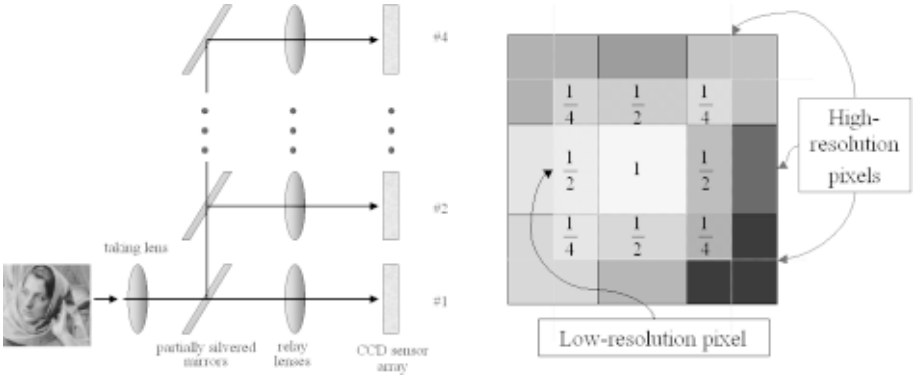

Figure 1. Low-resolution image formation (left) and blur matrix (right).

Figure 2. Low-resolution image (left) and high-resolution image (right).

Another approach for the reconstruction of the high-resolution image is from the wavelet point of view, where we analyze the reconstruction process through multi-resolution analysis. The low-resolution images can be thought of as the low-frequency samples of f obtained by passing it through some low-pass filters. Thus the problem can be posed as reconstructing an image from given, multiple, low-frequency samples of f. To recover f, we deconvolve iteratively its high-frequency components hidden in the low-frequency samples. Our iterative process decomposes the image obtained in the previous iteration into different frequency components in the wavelet transform domain, and then adds them to the new iteration to im-

Continued on page 10.

Hyperspectral image coding for remote-sensing applications

Hyperspectral images have been successfully used for image classification and segmentation in remote sensing: in applications of supervised environment monitoring or geographic information systems, for instance. Nevertheless, one facet of the awkwardness of using hyperspectral images is their huge size. A typical image (covering a small region of a few kilometers, for example) has millions of pixels, with each pixel represented by several bands. Further, high resolution may be used for each pixel band (e.g. 24bpp).

Since not all the information contained in an image is actually needed to properly classify it with a high accuracy, recent studies have looked at how much hyperspectral images may be compressed without affecting the classification percentage.[1] This is the issue we will consider here.

Image coding

Figure 1 shows a simplified block diagram of the components of the encoder in a typical, lossy, compression system: first, a transform is applied in order to obtain a set of coefficients that are un-correlated and that include some with higher energy compactness. Second, a quantization stage removes information considered unnecessary. Third, an entropy coding scheme is applied to further compress the data. The overall goal is to produce a recovered image *I'* as close as possible to the original image *I* while preserving the bit rate for *I** as low as possible.

This short survey provides an experimental comparison of five image compression algorithms applied to hyperspectral images. The first is JPEG standard, used for a number of years and no longer state-of-the-art. The other four methods rely on a wavelet transform as the first step of the coding system. Subband image coding is an efficient method of image compression because subbands of the same level have little interband correlation; however, some spatially-varying interband energy dependence is often visible across the levels of the wavelet pyramid. The first two of these four methods are motivated by such statistically significant dependence and yield an embedded encoder. In the other two methods the subbands are encoded separately, not yielding an embedded encoding.

The first embedded method, EZW,[2] directly employs a model of the statistical dependencies between levels in the wavelet transform, and then encodes the binary symbols with an arithmetic coder. The second embedded method, SPIHT,[3] avoids the expensive arithmetic coder by introducing block symbols along the tree of levels. The first non-embedded method, LVQ,[4] groups the wavelet-transformed coefficients of the same subband into vectors, which are then quantized by means of lattices: the indices of the resulting lattice points are then arithmetically encoded. The JasPer implementation of JPEG2K performs a scalar-quantization on the wavelet coefficients and then arithmetically encodes them.

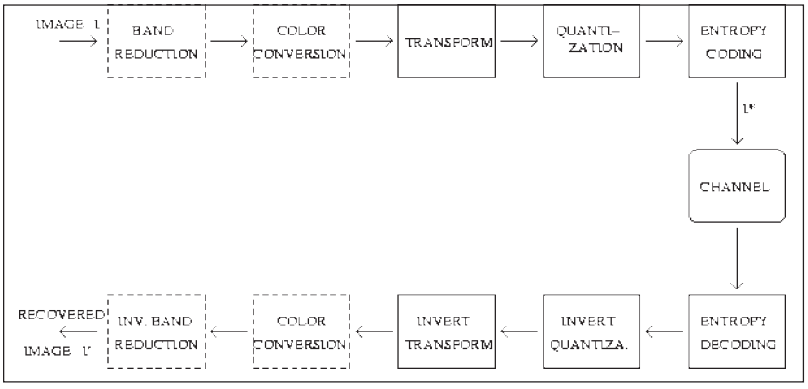

Figure 1. Components of a typical image coding system.

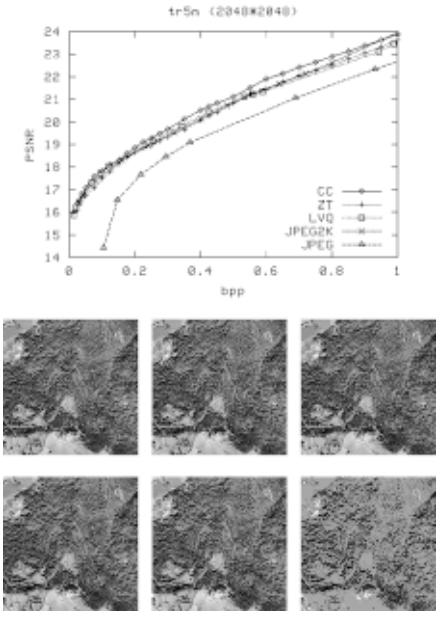

Figure 2. Top: Rate-distortion curve for grayscale CASI image using the different compression methods. Bottom (from top left to bottom right): original (uncompressed); and EZW; SPIHT; LVQ; JPEG2K; and JPEG all compressed at 190:1.

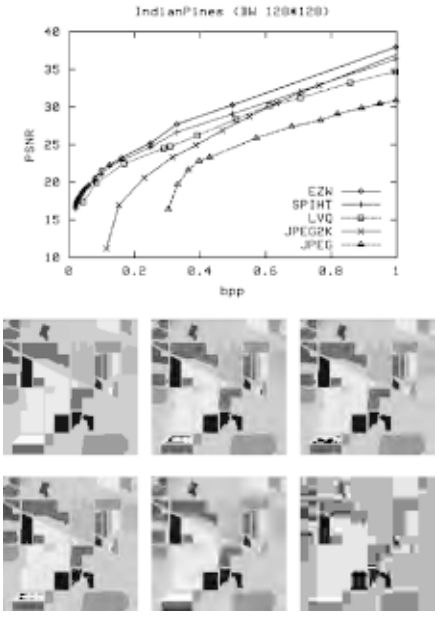

Figure 3. Top: Rate-distortion curve for AVIRIS Indian Pines Ground Truth image using the different compression methods. Bottom: (from top left to bottom right): original (uncompressed); and EZW; SPIHT; LVQ; JPEG2K; and JPEG all compressed at 25:1.

Experimental results and conclusions

Variants of the EZW, SPIHT and LVQ methods have been implemented. The results produced by JPEG and JPEG2K are also provided. See Figures 2 and 3 for, respectively, a grayscale CASI (compact airborne spectrographic imager) image and an AVIRIS (airborne visible infrared imaging spectrometer)

Continued on page 8.

Trends in lossless image compression by adaptive prediction

Image compression is gaining ever-increasing attention because of the huge amount of data to be archived and/or transmitted. Compression methods can be either reversible, i.e., *lossless*[1,2] or irreversible (*lossy*), depending on whether distortion is introduced or not. In the medical field and in remote sensing applications, the original quality must often be thoroughly preserved. Hence, considerable research efforts have been spent in the development of lossless image-compression techniques.

The first standard was the lossless version of JPEG. A new standard has been recently released, named JPEG-LS, based on an adaptive non-linear prediction and exploiting context modeling followed by Golomb-Rice entropy coding. A similar context-based algorithm named CALIC has also been recently proposed[1]. Part I of the JPEG2000 image-coding standard foresees a lossless mode, based on reversible integer wavelets, capable of providing a scalable bit stream that can be decoded up to the lossless level. Besides integer transforms[3], *differential pulse code modulation* (DPCM) algorithms are suitable for lossless compression.

Advanced compression algorithms

Advanced DPCM methods have two major components: adaptive prediction and adaptive entropy coding.[2] Current research can be divided into two categories: the first aims at achieving better compression performance than JPEG-LS and CALIC, while keeping computational complexity reasonably low. The second aims at determining the ultimate compression that can be achieved regardless of computational complexity.[4-6] This issue is relevant to investigate the best trade-off between computation and performance, in view of the ever-increasing processing capabilities of commercial hardware systems.

Given a causal neighborhood (set of pixels that have previously been scanned) the simplest predictor takes a linear combination of the pixel values lying within it, with coefficients optimized to yield minimum MSE (MMSE) over the whole image. Such a prediction, however, is optimum only for stationary signals. Hence, a space-varying prediction rule must be envisaged. Although broadly labeled as adaptive prediction, two approaches are feasible: a strictly adaptive DPCM (ADPCM), in which the coefficients of an MMSE predictor are continuously recalculated from the incoming data, and a classified DPCM, in which a training phase is aimed at recognizing some statistical classes of pixels and at calculating an optimized predictor for each class. Such predictors are adaptively combined (as, in the limit case, the output is switched to just one of them), to attain the best prediction. This will be referred to as adaptive combination/switching of adaptive predictors (ACAP/ASAP). The latter yields a crisp adaptive DPCM,[6] whereas the former can be regarded as a fuzzy adaptive DPCM.[5]

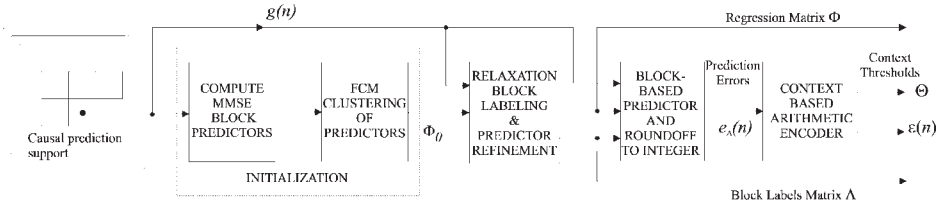

Figure 1. Flowchart of Relaxation-Labelled Prediction (RLP) DPCM encoder.

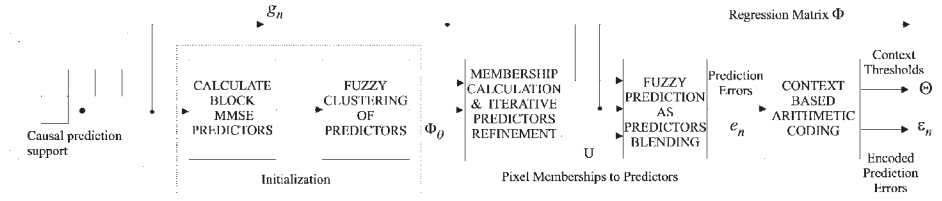

Figure 2. Flowchart of the Fuzzy-logic Matching Pursuits (FMP) DPCM encoder.

Another notable feature of all the advanced methods[1,3-6] is statistical context modelling for entropy coding. Prediction errors are arranged into a predefined number of homogeneous classes based on their spatial context. If such classes are statistically discriminated between, then the entropy of a context-conditioned model of residues will be lower than that of a stationary memoryless model of the decorrelated source. The context function used[5,6] is defined and measured on residues lying within a causal neighborhood—possibly larger than the prediction support—as the weighted RMS value of prediction errors (RMSPE).[7]

DPCM by relaxation-labelled prediction

The first method[6] is based on a classified linear-regression prediction followed by context-based arithmetic coding of the outcome residuals. Images are partitioned into blocks, typically 8×8, and an MMSE linear predictor is calculated for each block. Given a preset number of classes, a clustering algorithm produces an initial guess of a user-specified number of classified predictors to be fed to an iterative labelling procedure that classifies pixel blocks simultaneously refining the associated predictors. All predictors are transmitted along with the label of each block. Prediction errors are context-arithmetic encoded. Figure 1 shows the flow-chart of the encoder.

DPCM by fuzzy matching-pursuit prediction

Matching pursuit (MP) is an iterative method that expands a signal by using an over-complete dictionary of non-orthogonal functions. Although MP has been employed mostly for video coding, its original formulation is quite general. We assume that the MMSE adaptive predictor at the current pixel is expressed as a series expansion of a dictionary made of a number of predictors fitting the different classes of features occurring within the image.

The ACAP paradigm underlies the development of the fuzzy matching pursuit (FMP) prediction.[5] Initialization is identical to that of RLP. In the iterative refinement procedure, pixels are given degrees of membership measuring the fitness of prediction for each predictor, then predictors are recalculated from pixels depending on their degrees of membership. The fuzzy prediction is given by the sum of the outputs of each predictor weighted by the memberships of the current pixel to it. Thanks to the linearity of prediction, this approach is equivalent to approximating the optimum space-varying linear predictor at each pixel by projecting it onto a set of non-orthogonal prototype predictors capable of embodying the statistical properties of the image data. Figure 2 shows the flow-chart of the encoder.

Experimental results and comparisons

Several lossless algorithms have been com-

Continued on page 9.

Visual pattern coding of human-visual-system-based wavelets for image compression

The proliferation of digital media has motivated innovative methods for compressing digital images. The popular Joint Photographic Experts Group (JPEG) and Graphical Interchange Format (GIF) standards have been the prevailing methodologies in image compression in the past decade.[1] On the other hand, recent research in digital image compression has explored and improved the utility of the wavelet transform. Its success as a compression technique has prompted its inclusion in the JPEG2000 standard. In addition to the traditional wavelet transform, alternative wavelet-based compression schemes have shown great promise. In many applications requiring image compression, a human observer is the final receiver of the image information. Human visual system (HVS) properties must be taken into consideration to achieve quality reconstruction of images. Since more error can be tolerated at frequencies where the observer has lower sensitivity to noise, knowledge of the frequency response of a human observer can be used in the coding of bandpass signals.

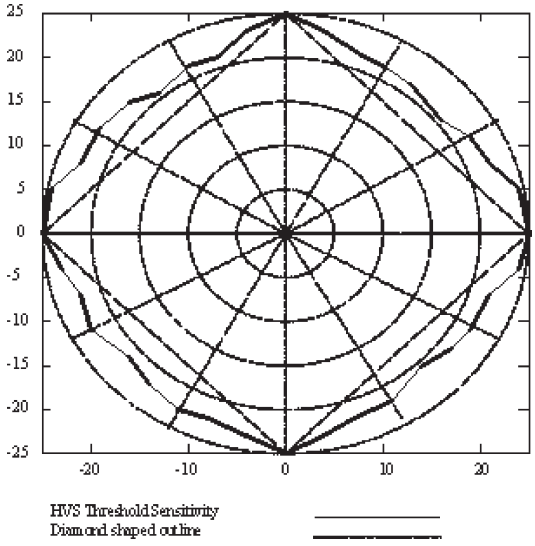

Figure 1. Diamond shape of HVS sensitivity.

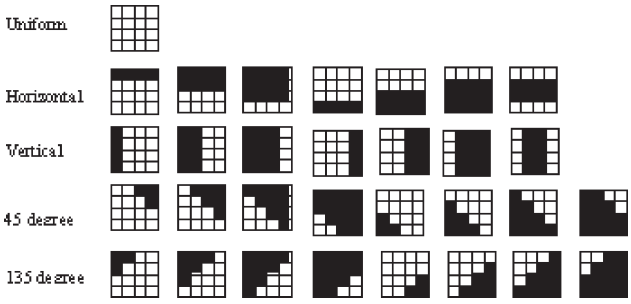

Figure 2. A set of visual patterns used in coding.

A wavelet-based video compression technique, which incorporates properties of human vision in the design of the compression system, may result in the high-quality reconstruction of images. In this article, we briefly describe a wavelet-based image compression technique that incorporates some of the human visual system (HVS) characteristics for the wavelet decomposition and bit allocation of sub-band images. The proposed method is essentially a perceptually-efficient form of a two-level vector quantization (VQ) that preserves the underlying edge geometries in the high frequency signals at very low coding rates.[2] Unlike the traditional VQ, the proposed method does not depend on a training set.

The purpose of sub-band decomposition in image coding is twofold: the first aim is to compact energy, the second is to make the divisions into sub-bands in a way such that all data represented in the same sub-band is, visually, equally important. The latter allows for a weighting of the quantization errors according to the sensitivity of the HVS, and supports progressive transmission. It is well known that humans perceive horizontal and vertical frequencies better than oblique ones. This is probably due to the dominance of horizontal and vertical structures in the environment. The partitioning into approximately octave bandwidths of the channels of the HVS motivates a hierarchical, dyadic, sub-sampling scheme. If we approximate the iso-sensitivity curves in the 2D-frequency-sensitivity function of the HVS with diamond shapes, it becomes natural to do a diamond-shaped band splitting (Figure1). Quincunx sampling in the spatial domain is compatible with diamond-shaped frequency areas. This first partitioning requires a two-dimensional filtering, which is the most computationally costly part of the scheme. All subsequent steps can be performed using 1-D filtering. This decomposition preserves the diamond shape of the lowest sub-band, and can be recursively performed until the desired number of sub-band decompositions has been achieved.[3]

To maximize perceived image quality at low bit rates, a large fraction of the available bits must be allocated to the lowest frequency sub-band where most of the image energy is concentrated. In part, the spatial sharpness is located in the higher-frequency bands. Although the energy is low for the high-frequency bands, they contain many perceptually-relevant image details and must be coded very effectively, preserving the basic features at a low rate. Due to the highly-structured and sparse nature of the signal in the non-dominant sub-bands, a perceptually-efficient form of quantization must be used to preserve the underlying edge geometries in the high-frequency signals at very low coding rates.

We propose a pattern-based coding method, where a small set of local geometric patterns is used to code an image. The design of the block patterns is inspired by edge-related features of the high-frequency sub-bands. The HVS-adapted sub-bands are then coded separately. The image is first divided into 4×4 blocks and each is then replaced by one of the finite number of visual patterns that best matches its features (Figure 2). Critical to the success of our approach is the frequent use of a spatial pattern: a uniform pattern of constant intensity to reproduce image blocks of near-constant intensity. The use of a uniform pattern adds some distortion to the reconstructed image, but this distortion will be among the wavelet coefficients with the smallest absolute values. After the inverse wavelet transform, these smallest coefficients correspond to scaled wavelets with low contrast: and have the least visual impact on the image. The number of patterns used for a particular sub-band image effects the quality of the reconstruction in that sub-band. A larger number of patterns will generally produce a higher quality reproduction. A larger look-up table will also requires more bits to be transmitted.

Since all the filtering in HVS-based wavelet decomposition is performed along the diagonals, the quantization artifacts are therefore found to be oriented along the diagonals where the HVS is least sensitive. As a result, the quan-

Continued on page 10.

Differential sensing of vibration for high-quality restoration of motion-blurred images

Continued from cover

each frame occurs over a different portion of the sine wave motion.

The small LED image is close to being an impulse function. Therefore, the obtained vibrated images are close to being the vibration LSF. This provides an opportunity to compare the LSF calculated from the sensor signals with that derived from the images. Both sensor and image data were downloaded into a PC and the restoration was performed using MATLAB. In Figure 2, examples of original vibrated LED images, LSFs derived from the sensor signal and image, and restored LED images are presented. The original images are very blurred by the vibrations, with blur size of 35 pixels. This is of course much greater than the image size of the LED (two pixels).

From the LSF curves in Figure 2, it can be seen that differential sensing with two accelerometers gives very accurate results for considerably different LSF shapes. The mean squared error of the measurement for these examples is in the range of 0.16–0.47%. Such accuracy can rarely be obtained from image data, except for images with well-defined sharp object boundaries. The reported accuracy of LSF detection for the blind restoration algorithms is in the range of 1.5–27% for single-frame-based techniques, and 2–10% for frame-sequence-based techniques. As a result, as can be seen in the examples, the restoration of the vibration-blurred images based on the differentially-measured motion function is very accurate and is essentially total.

Boris Likhterov and Norman S. Kopeika
Ben-Gurion University of the Negev
Electrical Engineering Department
POB 653, Beer-Sheva 84105, Israel
E-mail: lichtrov@ee.bgu.ac.il

Reference

1. B. Likhterov and N. S. Kopeika, *Differential Sensing of Vibration for High Quality Restoration of Motion-Blurred Images,* **Optical Engineering 41** (11), pp. 2970-2974, November 2002.

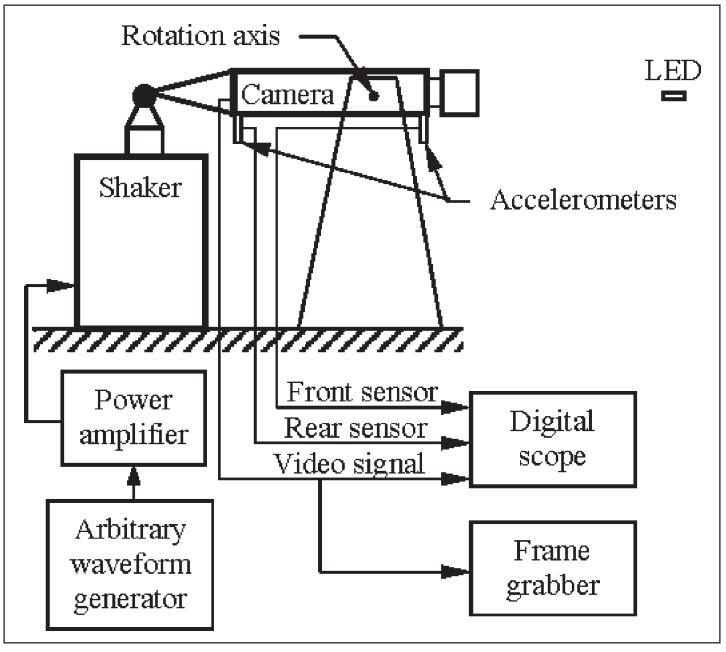

Figure 1. Experimental setup for differential vibration sensing.

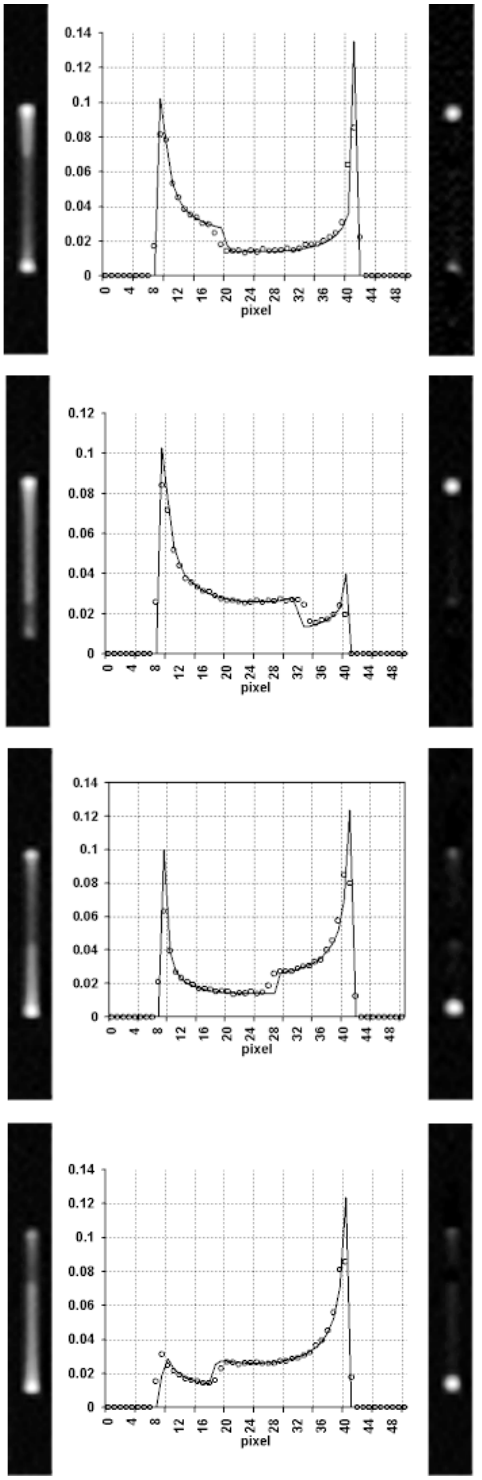

Figure 2. Four examples of LED image restoration with different LSFs. Left side: original vibration-blurred images. Graphs: LSF measured with differential sensing scheme (solid line) and calculated from the image (circles). Right side: restored images.

Hyperspectral image coding for remote-sensing applications

Continued from page 4.

Indian Pines Ground Truth image. In both figures, the rate-distortion curve is shown at the top and the original in the top left. Then, continuing from top left to bottom right, are images compressed at 190:1 (Figure 1) and 25:1 (Figure 2) using EZW, SPIHT, LVQ, JPEG2K and JPEG.

Although the four wavelet-based methods present important structural differences, experimental results carried out on several corpuses of images show that all the techniques produce approximately the same performance from very-low bit rate (320:1) to low bit rate (8:1). In fact, the rate-distortion curves for EZW and for SPIHT overlap most of the time. This seems to indicate that statistical modeling of the dependencies within transformed images is the key to state-of-the-art still-image coding.

For some images, when the bit rate gets close to 1bpp, LVQ loses some of its performance, although it is still above JPEG performance. For images of medium or large size, JPEG2K also provides comparable performance for all bit rates; for smaller sizes, and for very-low bit rates, its performance degrades.

From a computational complexity perspective, EZW, LVQ and JPEG2K need an arithmetic coding step. SPIHT avoids this expensive step, and is therefore more suitable for a real-time implementation.

Table1. A summary of the reviewed encoding methods.

Method	Transform	Quantization	Entropy Coding
JPEG	2-d DCT	Scalar	Huffman
EZW	Wavelet	---	Arithmetic
SPIHT	Wavelet	---	---
LVQ	Wavelet	Vector	Arithmetic
JPEG2K	Wavelet	Scalar	Arithmetic

Joan Serra-Sagrista
Computer Science Department, ETSE
Universitat Autonoma Barcelona
E-08193 Barcelona (SPAIN)
E-mail: Joan.Serra@uab.es
http://ccd-hyper.uab.es

References

1. J. Minguillon, J. Pujol, J. Serra-Sagrista, I. Ortuno, and P. Guitart, *Adaptive lossy compression and classification of hyperspectral images,* **Proc. SPIE 4170,** pp. 214-225, 2001.
2. J. M. Shapiro, *Embedded image coding using zerotrees of wavelet coefficients,* **IEEE Trans. on Signal Processing 41,** pp. 3445-3462, December 1993.
3. A. Said and W. A. Pearlman, *A new fast and efficient image codec based on set partitioning in hierarchical trees,* **IEEE Trans. on Circuits and Systems for Video Technology 6,** pp. 243-250, June 1996.
4. J. Serra-Sagrista, D. Gavilan, and J. Minguillon, *Analysis of compression methods applied to hyperspectral images,* **Proc. SPIE 4885,** 2002.

Security-printing authentication using digital watermarking

Continued from page 12.

authentication processes. For performance evaluation, we have applied the common Stirmark attack tests to our digital watermarking system. These consist of approximately 90 different types of image manipulation or attack. Table 1 illustrates some sample authentication results obtained against the various Stirmark image attacks. Moreover, we have also included our own DAD attacks that are relevant to security printing applications and proved that the technique was able to survive the "unknown" types of print-scan attacks.

The proposed authentication system can solve the problem of photograph-substitution frauds, such that if the attacker tries to change the photograph, the verifier would be unable to extract the correct personal ID from the fake bearer's photograph. As this water-marking system mainly involves a simple software implementation, it can be easily integrated with any PC systems, with an input scanner the only hardware needed.

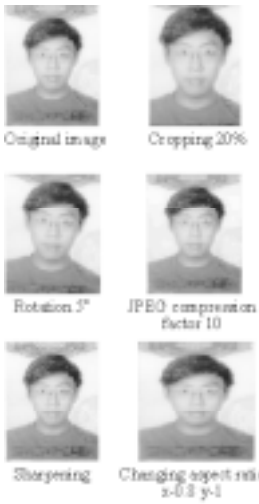

Figure 3. Sample Stirmark attacks on original image.

Table 1. Sample results of Stirmark tests for the watermarked passport photograph.

Attacks	Image PSNR(dB) under attacks	Authentication Result (YES or NO)
Cropping 75%	NA	YES
17 row 5 columns removed	NA	YES
3x3 Media Filtering	27.36	YES
Frequency Mode Laplacian removal	33.37	YES
Gaussian filtering 3x3	31.93	YES
JPEG Compression of factor 10	30.99	YES
General linear transformation	NA	YES
Scaling 0.5	NA	YES
Scaling 2.0	NA	YES
Change aspect ratio	NA	YES
Rotation with cropping 0.25° or >1°	NA	YES
Rotation with cropping 0.5°-1°	NA	NO
Sharpening 3x3	23.45	YES
Shearing 1%	NA	YES
Shearing 5%	NA	NO
Color reduction	NA	YES
Stirmark with randomisation and bending	21.75	NO

Anthony T. S. Ho, Jun Shen, Hong Pew Tan,* and Jerry Woon*
Division of Information Engineering
School of Electrical and
Electronic Engineering
Nanyang Technological University
Singapore 639798
E-mail: etsho@ntu.edu.sg

*DataMark Technologies Pte Ltd
100 Jurong East Street 21
Singapore Technologies Building
Singapore 609602
htpp://www.datamark-tech.com

References

1. J. Mercer, **Authentication News 5** (9/10), 2001.
2. *Security Needs for Passports,* **Authentication News 7** (3/4), May/June 2001.
3. A. T. S. Ho, J. Shen, and S. H. Tan, *Character-embedded watermarking algorithm using the fast Hadamard transform for satellite images,* **Proc. SPIE 4793,** 2002.
4. A. T. S. Ho, J. Shen, and S. H. Tan, *Robust digital image-in-image watermarking algorithm using the fast Hadamard transform,* **Proc. SPIE 4793,** 2002.

Trends in lossless image compression by adaptive prediction

Continued from page 5.

Table 1. Bit rates (in bit/pel) needed to encode the test images by several reversible compression methods: with the exception of JPEG-LS employing Golomb-Rice entropy coding, all methods use arithmetic coding. Best result for each image emphasized in boldface. TMW results, where unavailable, have been replaced with the best available ones (those of FMP, except for X-ray) to compute the average on the last row.

Image	FMP	RLP	TMW	CALIC	S&P	JPEG-LS	L-J2K
Airplane	3.66	3.71	**3.60**	3.74	3.90	3.82	4.02
Baboon	**5.69**	5.74	5.73	5.88	5.92	6.04	6.11
Balloon	2.68	2.73	**2.65**	2.83	2.96	2.90	3.04
Barb	**3.93**	4.03	4.08	4.41	4.51	4.69	4.61
Barb2	**4.33**	4.39	4.38	4.53	4.70	4.69	4.80
Board	**3.35**	3.41	n.a.	3.56	3.81	3.68	3.78
Boats	**3.60**	3.68	3.61	3.83	4.01	3.93	4.07
Bridge	5.62	5.66	**5.59**	5.68	5.80	5.79	6.00
Cameraman	4.11	4.18	**4.10**	4.19	4.46	4.31	4.56
Couple	3.51	3.56	**3.45**	3.61	3.87	3.70	3.94
Elaine	**4.40**	4.44	n.a.	4.80	4.87	4.90	4.95
Girl	**3.52**	3.61	3.67	3.77	3.95	3.93	4.07
Goldhill	4.28	4.31	**4.27**	4.39	4.54	4.48	4.61
Harbor	**4.36**	4.44	n.a.	4.44	4.72	4.49	4.78
Hotel	**4.14**	4.24	4.17	4.25	4.52	4.39	4.59
Lennagrey	**3.90**	3.96	3.91	4.11	4.16	4.24	4.31
Noisesquare	**5.24**	5.26	5.54	5.44	5.55	5.68	5.65
Peppers	**4.02**	4.08	4.03	4.20	4.35	4.29	4.42
Shapes	1.17	1.30	**0.76**	1.14	2.13	1.21	1.93
Zelda	**3.64**	3.66	n.a.	3.86	3.89	4.01	4.00
AVIRIS (12b)	**6.17**	6.18	n.a.	6.32	6.38	6.37	6.41
Landsat TM	**4.47**	4.50	n.a.	4.54	4.63	4.65	4.80
X-Ray	1.28	**1.27**	n.a.	1.45	1.71	1.56	1.64
CAT (10b)	**2.53**	2.60	2.54	2.85	2.95	2.87	2.99
Average	**3.90**	3.96	3.91	4.08	4.26	4.19	4.34

pared with the RLP and FMP encoders. Three are advanced algorithms established in the literature.[1,3,4] The last two entries are the new standard JPEG-LS and the lossless version of JPEG 2000 (L-J2K). All the methods are causal DPCMs, except S&P and L-J2, which use integer wavelets. A test set comprising widely-known grayscale images was used. Table 1 reports bit rates on disk—including overhead information—in bits per pixel.

FMP outperforms all the other methods on average: only TMW is comparable. The computational cost of the latter, however, is prohibitive, due to the massive training necessary. Results of FMP are impressive both on a homogeneous image, like the X-ray, and on a heterogeneous one, like *Baboon*. Especially on *Barb*, which comes from interlaced video, FMP exhibits outstanding performance with respect to all the other schemes. The parameters of FMP have been optimized for performance on *Lennagrey*. Although slightly poorer than FMP on the whole, RLP achieves the best result on the X-ray image.

Conclusions

This article describes two advanced approaches to lossless image compression based on adaptive prediction. Their superior performance depends on their ability to capture the most relevant features of the data, which are then exploited to make predictions that are locally adaptive: either through the switching of a number of fitting prototype predictors (ASAP protocol) or by blending of the output of such predictors based on fuzzy-logic rules (ACAP protocol). In both cases, context modelling of prediction residues enhances entropy coding. Experiments have shown that the proposed adaptive DPCM schemes encompass the most advanced methods available, both in the literature, and among standards. Although RLP performs slightly less well than FMP, its feature of real-time decoding is highly valuable in application contexts, since an image is usually encoded only once, but decoded many times.

Bruno Aiazzi,* Luciano Alparone,† and Stefano Baronti*
*IFAC-CNR: Institute of Applied Physics *N. Carrara*
Via Panciatichi, 64
50127 Florence, Italy
E-mail: {aiazzi, baronti}@ifac.cnr.it
†DET: Department of Electronics and Telecommunications
University of Florence
Via Santa Marta, 3
50139 Florence, Italy
E-mail: alparone@det.unifi.it

References

1. X. Wu and N. Memon, *Context-based, adaptive, lossless image coding,* **IEEE Trans. Commun. 45** (4), pp. 437-444, 1997.
2. B. Carpentieri, M. J. Weinberger, and G. Seroussi, *Lossless compression of continuous-tone images,* **Proc. of the IEEE 88** (11), pp. 1797-1809, 2000.
3. A. Said and W. A. Pearlman, *An image multiresolution representation for lossless and lossy compression,* **IEEE Trans. Image Processing 5** (9), pp. 1303-1310, 1996.
4. B. Meyer and P. Tischer, *TMW-a new method for lossless image compression,* **Proc. IEEE Int. Picture Coding Symposium,** Berlin, Germany, pp. 533-538, 1997.
5. B. Aiazzi, L. Alparone, and S. Baronti, *Fuzzy logic-based matching pursuits for lossless predictive coding of still images,* **IEEE Trans. Fuzzy Systems 10** (4), pp. 473-483, 2002.
6. B. Aiazzi, L. Alparone, and S. Baronti, *Near-lossless image compression by relaxation-labelled prediction,* **Signal Processing 82** (11), pp. 1619-1631, 2002.
7. B. Aiazzi, L. Alparone, and S. Baronti, *Context modeling for near-lossless image coding,* **IEEE Signal Processing Lett. 9** (3), pp. 77-80, 2002.

Reconstruction of high-resolution images from low-resolution images

Continued from page 3.

prove the approximation.

***Raymond H. Chan, *P Russ K. Ling, and †Michael K. Ng**
*Department of Mathematics
The Chinese University of Hong Kong
Shatin, Hong Kong
E-mail: rchan@math.cuhk.edu.hk
†Department of Mathematics
The University of Hong Kong
Pokfulam Road, Hong Kong
E-mail: mng@maths.hku.hk

References

1. N. Bose and K. Boo, *High-Resolution Image Reconstruction with Multisensors*, **International Journal of Imaging Systems and Technology 9,** pp. 294-304, 1998.
2. R. Chan, T. Chan, L. Shen, and Z. Shen, *Wavelet Algorithms for High-Resolution Image Reconstruction,* **The Chinese University of Hong Kong, Department of Mathematics, Research Report #2000-20.** To appear in **SIAM Journal on Scientific Computing**.
3. M. Ng, R. Chan, T. Chan, and A. Yip, *Cosine Transform for High-Resolution Image Reconstruction,* **Linear Algebra and its Applications 316,** pp. 89-104, 2000.
4. R. Chan and R. Ling, *Reconstruction of High Resolution Image from Movie Frames,* **The Chinese University of Hong Kong, Department of Mathematics, Research Report #2002-30.**

Visual pattern coding of human-visual-system–based wavelets

Continued from page 6.

tization artifacts are less noticeable than the standard wavelet quantization effects, which are also aligned horizontally and vertically. In terms of subjective quality, HVS is superior to JPEG2000 for all images. JPEG2000 has a tendency to smooth the image, thereby losing texture and depth information. Our HVS compression scheme retains these details, thus delivering subjectively-better image reconstruction. In terms of PSNR, the HVS-based system usually outperforms JPEG2000 by 1 to 3 dB. JPEG2000 only exceeds the HVS-based system at the highest bit rate on images with large areas of uniformity. For these images, JPEG2000 has the benefit of arithmetic coding. HVS compression would presumably surpass JPEG2000 in all cases with the addition of an entropy coder.

Dr Farhad Keissarian
Department of Electrical Engineering
UAE University
Al-Ain, PO Box 17555, UAE
E-mail: farhad.k@uaeu.ac.ae

References

1. A. N. Skodras, C. A. Christopoulos, and T. Ebrahimi, *Jpeg2000: The upcoming still image compression standard,* **Proc. 11th Portugese Conf. on Pattern Recognition,** pp. 359-366, May 2000.
2. T. O'Rourke and R. Stevenson, *Human visual system based wavelet decomposition for image compression,* **J. VCIP 6,** pp. 109-121, 1995.
3. F. Keissarian and M. F. Daemi, *Block pattern coding of HVS based wavelets for image compression,* **Proc. SPIE 4472,** pp. 424–432, August, 2001.

Tell us about your news, ideas, and events!

If you're interested in sending in an article for the newsletter, have ideas for future issues, or would like to publicize an event that is coming up, we'd like to hear from you. Contact our technical editor, Sunny Bains (sunny@spie.org) to let her know what you have in mind and she'll work with you to get something ready for publication.

Deadline for the next edition, 13.2, is:

31 January 2003: Suggestions for special issues and guest editors.

21 February 2003: Ideas for articles you'd like to write (or read).

18 April 2003: Calendar items for the twelve months starting June 2003.

CALENDAR

2003

SPIE's Photonics West
25-31 January
San Jose, California USA
http://spie.org/Conferences/Programs/03/pw/

International Conference in Image Problems: Iconics 2003
23-25 April
St. Petersburg, Russia
Sponsored by SPIE Russia
http://latonita.star.spb.ru/ImageCON/eng/

The PICS Conference
13-16 May
The Hyatt Regency Hotel
Rochester, NY
http://www.imaging.org/conferences/pics2003/

DPP 2003: International Conference on Digital Production Printing and Industrial Applications
18-23 May
The Hilton Barcelona Hotel
Barcelona, Spain
http://www.imaging.org/conferences/dpp2003/

6th International Conference on Quality Control by Artificial Vision
19-23 May
Gatlinburg, Tennessee USA
SPIE is a cooperating organization and will publish the Proceedings
http://www.ornl.gov/qcav2003

Biophotonics Pacific Rim - PIBM/MDM 2003: Third International Conference on Photonics and Imaging in Biology and Medicine 2003
8-11 June
Wuhan, China
SPIE will publish proceedings
http://www.hust.edu.cn/pibm2003

SPIE's Visual Communications and Image Processing 2003
8-11July
Lugano, Switzerland
http://spie.org/conferences/calls/03/vc

SPIE's ITCom 2003 Information Technologies and Communications
7-11 September
Orlando, Florida USA
http://spie.org/conferences/calls/03/it

SPIE's Remote Sensing Europe
8-12 September
Barcelona, Spain
http://spie.org/conferences/calls/03/ers

NIP19: The I9th International Congress on Digital Printing Technologies
28 September -3 October
Hyatt Regency Hotel
New Orleans, Louisiana
http://www.imaging.org/conferences/nip19/

For More Information Contact
SPIE • PO Box 10, Bellingham, WA 98227-0010
Tel: +1 360 676 3290 • Fax: +1 360 647 1445
E-mail: spie@spie.org • Web: www.spie.org

Join the SPIE/IS&T Technical Group

...and receive this newsletter

This newsletter is produced twice yearly and is available only as a benefit of membership of the SPIE/IS&T Electronic Imaging Technical Group.

IS&T—The Society for Imaging Science and Technology has joined with SPIE to form a technical group structure that provides a worldwide communication network and is advantageous to both memberships.

Join the Electronic Imaging Technical Group for US$30. Technical Group members receive these benefits:

- *Electronic Imaging* Newsletter
- SPIE's monthly publication, ***oe****magazine*
- annual list of Electronic Imaging Technical Group members
- discounts on registration fees for IS&T and SPIE meetings, and on books and other selected publications related to electronic imaging.

People who are already members of IS&T or SPIE are invited to join the Electronic Imaging Technical Group for the reduced member fee of US$15.

Please Print ☐ Prof. ☐ Dr. ☐ Mr. ☐ Miss ☐ Mrs. ☐ Ms.

First (Given) Name _____ Middle Initial _____

Last (Family) Name _____

Position _____

Business Affiliation _____

Dept./Bldg./Mail Stop/etc. _____

Street Address or P.O. Box _____

City _____ State or Province _____

Zip or Postal Code _____ Country _____

Phone _____ Fax _____

E-mail _____

Technical Group Membership fee is $30/year, or $15/year for full SPIE and IS&T Members.

Amount enclosed for Technical Group membership **$** _____

❑ **I also want to subscribe to IS&T/SPIE's *Journal of Electronic Imaging* (JEI)** **$** _____ *(see prices below)*

Total $ _____

❑ **Check enclosed.** Payment in U.S. dollars (by draft on a U.S. bank, or international money order) is required. Do not send currency. Transfers from banks must include a copy of the transfer order.

❑ **Charge to my:** ❑ **VISA** ❑ **MasterCard** ❑ **American Express** ❑ **Diners Club** ❑ **Discover**

Account # _____ Expiration date _____

Signature _____
(required for credit card orders)

Reference Code: 3537

JEI 2003 subscription rates (4 issues):	**U.S.**	**Non-U.S.**
Individual SPIE or IS&T member*	$ 55	$ 55
Individual nonmember and institutions	$255	$275

Your subscription begins with the first issue of the year. Subscriptions are entered on a calendar-year basis. Orders received after 1 September 2003 will begin January 2004 unless a 2003 subscription is specified.

One journal included with SPIE/IS&T membership. Price is for additional journals.

Send this form (or photocopy) to:
SPIE • P.O. Box 10
Bellingham, WA 98227-0010 USA
Tel: +1 360 676 3290
Fax: +1 360 647 1445
E-mail: membership@spie.org

Please send me:
☐ **Information about full SPIE membership**
☐ **Information about full IS&T membership**
☐ **Information about other SPIE technical groups**
☐ **FREE technical publications catalog**

Electronic Imaging

The *Electronic Imaging* newsletter is published by SPIE—The International Society for Optical Engineering, and IS&T—The Society for Imaging Science and Technology. The newsletter is the official publication of the International Technical Group on Electronic Imaging.

Technical Group Chair	Arthur Weeks
Technical Group Cochair	Gabriel Marcu
Technical Editor	Sunny Bains
Managing Editor/Graphics	Linda DeLano

Articles in this newsletter do not necessarily constitute endorsement or the opinions of the editors, SPIE, or IS&T. Advertising and copy are subject to acceptance by the editors.

SPIE is an international technical society dedicated to advancing engineering, scientific, and commercial applications of optical, photonic, imaging, electronic, and optoelectronic technologies.

IS&T is an international nonprofit society whose goal is to keep members aware of the latest scientific and technological developments in the fields of imaging through conferences, journals and other publications.

SPIE—The International Society for Optical Engineering, P.O. Box 10, Bellingham, WA 98227-0010 USA. Tel: +1 360 676 3290. Fax: +1 360 647 1445. E-mail: spie@spie.org.

IS&T—The Society for Imaging Science and Technology, 7003 Kilworth Lane, Springfield, VA 22151 USA. Tel: +1 703 642 9090. Fax: +1 703 642 9094.

EIONLINE

Electronic Imaging Web Discussion Forum

You are invited to participate in SPIE's online discussion forum on Electronic Imaging. To post a message, log in to create a user account. For options see "subscribe to this forum."

You'll find our forums well designed and easy to use, with many helpful features such as automated email notifications, easy-to-follow 'threads,' and searchability. There is a full FAQ for more details on how to use the forums.

Main link to the new Electronic Imaging forum:

`http://spie.org/app/forums/tech/`

Related questions or suggestions can be sent to `forums@spie.org`.

SPIE The International Society for Optical Engineering

Security-printing authentication using digital watermarking

Security-printing products are commonly found in many important day-to-day applications ranging from identity cards and driving licenses to certificates and passports. Many security documents are subject to fraudulent reproduction, adulteration and theft. Attempted frauds include total book counterfeiting, photograph substitution, page substitution, and expiry-date tampering. For example, photograph substitution accounts for about two-thirds of passport fraud.[1] A great deal of effort and research has been channelled into preventing such fraud.[2] Most of this relies on the physical construction of the photograph. For instance: for some driving licenses, the security printing process involves placing a security laminate over the bearer's digitized photograph. However, such features can still be easily attacked and illegally reproduced.

A simple yet secure approach to prevent photograph-substitution fraud is to provide a digital linkage between the bearer's photograph and his/her personal information. Our technique aims to establish this linkage using a novel, hybrid digital watermarking system. The process involves embedding the personal information (for example, owner's ID) as an invisible watermark into the owner's photograph. During the authentication process, the embedded information is extracted from the digitized photograph and compared with the personal ID printed on the security document. If a match between these IDs can be found, the document is confirmed as a true copy, otherwise it is counterfeit.

A personal ID can contain several characters that are formatted into a random bit stream. This bit stream is inserted into various frequency coefficients in several sub-blocks of an orthogonal transform such as a Discrete Cosine Transform (DCT) or Hadamard Transform (HT) of the original photograph.[3,4] The watermarked photograph can then be printed onto the security document. In the authentication process, the security document is first scanned into a computer. The watermarking system then extracts the hidden watermark information from the digitized photograph. The digital watermark embedding and authentication process are shown in Figure 1.

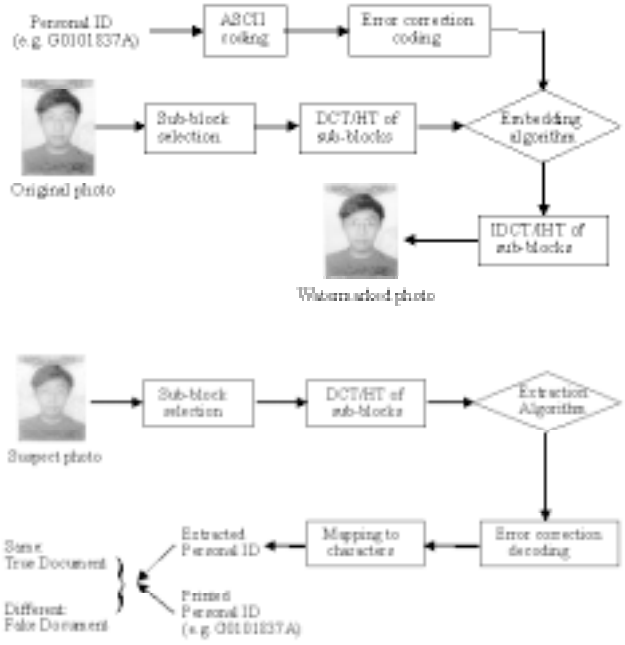

Figure 1. Watermark embedding (top) and authentication (bottom) process for security document application.

The entire operation involves a print-scan or digital–analogue-digital (DAD) conversion process that differs significantly from the traditional digital watermarking applications of copyright protection and authentication (which mainly focus in the digital domain). With this technique, a printed hardcopy with an invisible embedded watermark can be retrieved. This offers many potential business opportunities and applications for security documents, such as driving licenses, identity and credit cards. The print-scan or DAD process is illustrated in Figure 2.

The main performance criterion for any digital watermarking technique is its watermark robustness against various types of malicious image attacks or manipulations that attempt to destroy it. These attacks may include rotation, translation, scaling cropping, resam-pling, filtering, format conversion and JPEG compression. Moreover, the data integrity of the watermarked image should not suffer any degradation that is apparent to the naked eye. For commercial exploitation, the watermarking algorithm should provide ease of implementation and not be computationally intensive during the watermarking embedding and

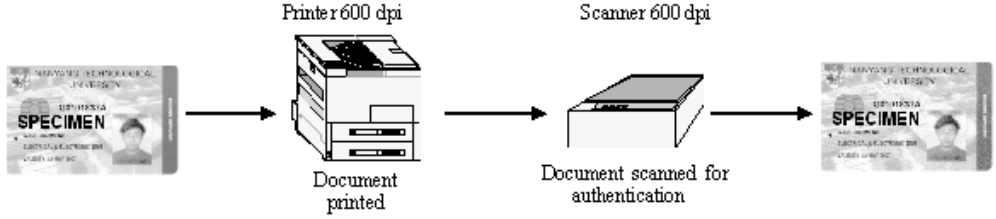

Figure 2. Digital-analogue-digital conversion process or print-scan process.

Continued on page 8.

SPIE Society of Photo-Optical Instrumentation Engineers

P.O. Box 10 • Bellingham, WA 98227-0010 USA

Change Service Requested

DATED MATERIAL

Non-Profit Org.
U.S. Postage Paid
Society of
Photo-Optical
Instrumentation
Engineers